Optics Letters

Spatio-temporal enhancement of Raman-induced frequency shifts in graded-index multimode fibers

AMIRA S. AHSAN* AND GOVIND P. AGRAWAL

Institute of Optics, University of Rochester, Rochester, New York 14627, USA
**Corresponding author: aahsan@ur.rochester.edu*

Received 21 February 2019; revised 12 April 2019; accepted 24 April 2019; posted 25 April 2019 (Doc. ID 360613); published 16 May 2019

We investigate the impact of intrapulse Raman scattering and third-order dispersion on the propagation of a pulsed optical beam inside graded-index (GRIN) fibers by solving an effective nonlinear Schrödinger equation that includes the spatial self-imaging effects through a periodically varying effective mode area. Numerical simulations are used to show that the Raman-induced frequency shift of the shortest fundamental soliton, created after the fission process, is enhanced considerably inside GRIN fibers compared to single-mode fibers for the same value of the soliton order. We also discuss the role of spatial-width contraction during each self-imaging cycle on the Raman-induced frequency shifts.

https://doi.org/10.1364/OL.44.002637

Recently, there has been a resurgence of interest in multimode fibers, partially motivated by their applications in space-division multiplexing [1]. This has led to a notable effort to examine the spatiotemporal dynamics of nonlinear propagation in both the step-index and graded-index (GRIN) fibers [2,3]. Recent experiments have shown Kerr-induced spatial cleaning of pulsed beams inside GRIN fibers using picosecond as well as femtosecond pulses [4,5]. A new kind of spatiotemporal instability, known as geometric parametric instability and first studied in 2003 [6], has also been observed experimentally using GRIN fibers [7]. A temporal soliton composed of three modes of a GRIN fiber was observed in 2013 [8]. Theoretical work has also shown that solitons can form inside a GRIN medium [9–11]. Recent research has focused on the generation of a supercontinuum by exploiting various nonlinear effects inside GRIN fibers [12–15].

Several higher-order nonlinear and dispersion effects become quite important when ultrashort optical pulses are propagated inside single-mode fibers [16]. Among them, a continuous shift of the pulse's spectrum towards longer wavelengths, known as the soliton self-frequency shift, was studied as early as 1986 [17]. In recent years, such Raman-induced frequency shifts (RIFS) have been exploited to tune the wavelength of mode-locked lasers producing femtosecond pulses [18–20]. This technique requires the formation of higher-order solitons inside optical fibers and is particularly useful for generating radiation in the mid-infrared region [19]. Clearly, any technique that can enhance the magnitude of RIFS inside optical fibers would be useful for practical applications.

In this Letter we show that the RIFS of femtosecond pulses is enhanced considerably when the pulses are propagated through a multimode GRIN fiber in place of a single-mode fiber, while maintaining the same value of the soliton order at the input end. In what follows, we first present the effective nonlinear Schrödinger (NLS) equation governing propagation of pulses inside a GRIN fiber. We compare the temporal and spectral features for optical pulses evolving inside a GRIN fiber and a single-mode fiber. We then focus on the RIFS enhancement inside GRIN fibers and study how this enhancement depends on the specific parameters associated with a GRIN fiber.

The refractive index of a GRIN fiber varies radially in a parabolic fashion. Including also the contribution of the Kerr nonlinearity, it can be written as

$$n(\rho, I) = n_0(\omega)[1 - \Delta(\rho/a)^2] + n_2 I(\rho \le a), \quad (1)$$

where n_0 is the core index, a is the core radius, and $\Delta = (n_0 - n_c)/n_0$ with n_c standing for the cladding index. The Kerr nonlinearity of silica glass is incorporated through the Kerr coefficient n_2 and the local intensity I. When this form is used with Maxwell's equations, the resulting wave equation corresponds to a four-dimensional (4D) problem involving three spatial coordinates (x, y, z) and time t. In the case of a continuous-wave Gaussian beam, its solution exhibits the phenomenon of periodic self-imaging such that the beam-width oscillates along the fiber's length but recovers its input value at distances that are multiples of the self-imaging period $z_p = \pi a/\sqrt{2\Delta}$.

The important question is what happens when a pulsed Gaussian beam is launched into the same GRIN fiber. It was shown by Conforti *et al.* in 2017 that, under suitable conditions that hold well in practice for most GRIN fibers, the 4D pulse-propagation problem can be reduced to an effective 2D NLS equation involving only the z and t variables [21]. This equation incorporates the effects of spatial beam-width oscillations through a periodically varying effective-mode area but assumes that the temporal dynamics of the pulse do not affect these oscillations. We write the resulting NLS equation in a normalized form using the dimensionless variables [16]

$$\tau = t/T_0, \qquad \xi = z/L_D, \qquad U = A/\sqrt{P_0}, \quad (2)$$

where T_0 and P_0 are the width and the peak power of an input pulse, respectively, and $U(\xi, \tau)$ represents the slowly varying envelope of the evolving pulse. The dispersion length is defined as $L_D = T_0^2/|\beta_2|$, where β_2 is the group-velocity dispersion parameter at the pulse's central frequency ω_0. After including both the Kerr and the Raman contributions [16], the effective NLS equation takes the form

$$i\frac{\partial U}{\partial \xi} + \frac{1}{2}\frac{\partial^2 U}{\partial \tau^2} - i\delta\frac{\partial^3 U}{\partial \tau^3} + \frac{N^2}{f(\xi)} \times U(\xi,\tau)\int_0^\infty R(\tau')|U(\xi,\tau-\tau')|^2 \mathrm{d}\tau' = 0. \tag{3}$$

In the preceding equation, we assumed anomalous group-velocity dispersion ($\beta_2 < 0$) and included the effects of third-order dispersion through $\delta = \beta_3/(6|\beta_2|T_0)$. The soliton order N is defined as

$$N^2 = \gamma P_0 L_D, \qquad \gamma = \omega_0 n_2/(cA_{\mathrm{eff}}), \tag{4}$$

where the effective area A_{eff} appearing in the nonlinear parameter γ corresponds to the area at the input end of the fiber. Periodic variations of A_{eff} resulting from spatial self-imaging are included through the function $f(\xi)$ given by

$$f(\xi) = \cos^2(\pi q\xi) + C^2\sin^2(\pi q\xi), \qquad q = \frac{L_D}{z_p}. \tag{5}$$

The parameters z_p and C depend on the GRIN-fiber design and are defined as

$$z_p = \frac{\pi a}{\sqrt{2\Delta}}, \qquad C = \frac{(1-p)^{1/2}z_p}{\pi\beta_0 w_0^2}, \tag{6}$$

where w_0 is the input beam width and p is related to the input peak power P_0 as $p = n_2(\beta_0 w_0)^2 P_0/2n_0$. Physically, z_p represents the self-imaging period of the GRIN fiber and C governs the extent of beam compression during each cycle. It is worth noting that $C = 1$ amounts to setting $f(\xi) = 1$, which converts Eq. (3) into the standard NLS equation.

We solve Eq. (3) numerically using the well-known form of the nonlinear response function [16], $R(t) = (1 - f_R)\delta(t) + f_R h_R(t)$, where $f_R = 0.18$ is the fractional contribution of the delayed Raman response whose functional form $h_R(t)$ is taken from Ref. [22]. We solve Eq. (3) in the frequency domain using a technique that employs the fourth-order Runge–Kutta method in the interaction picture [23].

As the fission of higher-order solitons plays an important role in producing a large RIFS, it is important to consider how this process is affected by spatial beam-width oscillations occurring inside any GRIN fiber. For this purpose, we used numerical simulations to study the fission of a third-order soliton ($N = 3$) inside a GRIN fiber. We assume that a sech-shape pulse with a duration of 100 fs (full width at half-maximum) is launched into a GRIN fiber with a peak power such that it propagates as a third-order soliton. The self-imaging period z_p is typically ~1 mm, whereas the dispersion length L_D for a 100-fs pulse ($T_0 = 57$ fs) is ~10 cm. For the results shown in Figs. 1(a) and 1(b), we choose $q = L_D/z_P = 100$. We also set $C = 0.5$, which implies that the beam width is reduced to 50% of its input value in the middle of each self-imaging period. We used $\delta = 0.02$, the only other parameter that we needed to specify. As seen in part (a), the finite value of this parameter leads to the fission of the third-order soliton into three fundamental solitons within a fraction of the dispersion length. The spectral evolution

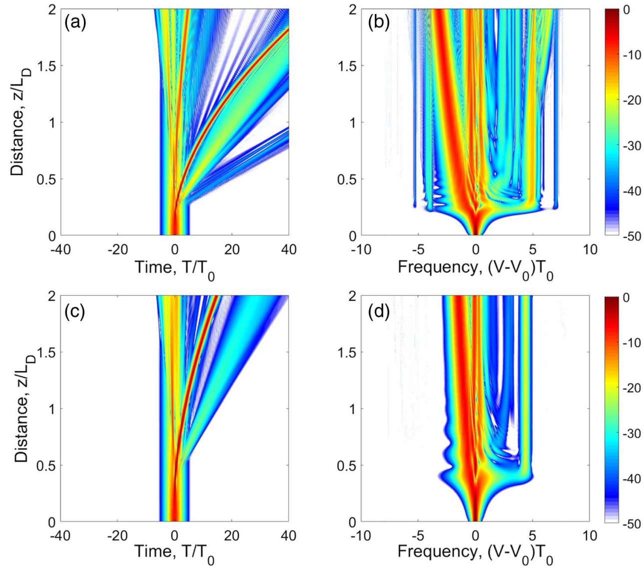

Fig. 1. Temporal (a) and spectral (b) evolution of a third-order soliton inside a GRIN fiber over a distance of $2L_D$ for $\delta = 0.2$, $C = 0.5$, and $q = 100$. Parts (c) and (d) show these features for a single-mode fiber under identical conditions except for $C = 1$ (no spatial oscillations). In all cases, intensity is color-coded on a 50-dB scale.

seen in part (b) shows that the pulse spectrum broadens considerably and develops a multi-peak structure after the fission.

To identify the impact of beam-width oscillations, we show in parts (c) and (d) the temporal and spectral evolutions of the same third-order soliton inside a single-mode fiber by setting $C = 1$. A direct comparison shows that the spatial width oscillations occurring inside a GRIN fiber have a huge impact in both the temporal and spectral domains. The reason is that width variations translate into peak-power variations (as pulse energy is conserved when losses are negligible), which translate into periodic refractive-index variations through the Kerr nonlinearity. The beam-width oscillations thus lead to two distinct physical mechanisms. First, the effects of self-phase modulation are enhanced in a periodic fashion as the pulse becomes more intense on a length scale governed by the self-imaging period (1 mm or less). Since a soliton cannot respond to such rapid variations, one can average over them, as discussed in Ref. [11]. The net result is the effective value of N becomes larger and is given by $\bar{N} = N/\sqrt{C}$. For the value of $C = 0.5$ used in Fig. 1, $\bar{N}$ exceeds 4, i.e., the third-order soliton behaves as a fourth-order soliton on average.

We can use this feature to understand the enhancement of the RIFS in part (b) of Fig. 1 compared to that in part (d). In both cases, the higher-order soliton breaks up into multiple fundamental solitons whose widths and the peak powers are governed by [16]

$$T_k = \frac{T_0}{2N + 1 - 2k}, \qquad P_k = (2N + 1 - 2k)^2\frac{P_0}{N^2}, \qquad k = 1 \ldots N. \tag{7}$$

However, we should replace N in this equation with the integer part of $\bar{N}$ in the case of a GRIN fiber. As a result, the width of each fundamental soliton created after the fission process is shorter in the case of GRIN fibers. Since the RIFS is larger for a shorter soliton, we expect it to be enhanced in the case of a GRIN fiber, when compared to a single-mode fiber with no spatial width oscillations. This is precisely what we observe in parts (b) and (d) of Fig. 1, where the most intense spectral peak shifts continuously toward the red side through the process of intrapulse Raman scattering. Such a red shift of solitons inside GRIN fibers has been observed in several experiments [24,25]. We quantify its magnitude in the next section.

Another noteworthy feature of Fig. 1(b) is the generation of multiple dispersive waves in the case of a GRIN fiber, in comparison to a single dispersive wave seen in part (d). It is a manifestation of the Kerr-induced index grating formed through periodic variations of the peak intensity. As is well-known, this grating enables the generation of a large number of dispersive waves by helping in satisfying a phase-matching condition [26,27]. By including terms up to third-order in dispersion, the frequency shift, $\omega = \omega_d - \omega_0$, is found to satisfy the following cubic polynomial [21,28]:

$$\frac{\beta_3\omega^3}{6}+\frac{\beta_2\omega^2}{2}-\delta\beta_1\omega=\frac{2\pi m}{z_p}+\frac{\gamma P_1}{2C}, \quad m=[-\infty,\infty], \tag{8}$$

where the $\delta\beta_1$ arises from a change in the group velocity of the soliton from its initial value [29]. Dispersive waves satisfying the condition in Eq. (8) were observed by Wright *et al.* in a 2015 work [28], where Eq. (8) was also discussed. Further, the experimental results were compared with numerical simulations based on an NLS equation similar to Eq. (3).

In Eq. (8), P_1 is the peak power of the shortest soliton formed after the fission process is completed. It can be estimated from Eq. (7) by taking $k = 1$ and replacing N with $\bar{N}$ in the case of a GRIN fiber. We write Eq. (8) in a normalized form using a new variable $\Omega = \omega T_0$:

$$2\delta_3\Omega^3 - \Omega^2 - \delta_1\Omega = 4\pi mq + (2\bar{N} - 1)^2, \tag{9}$$

where $\delta_1 = \delta\beta_1(L_D/T_0)$. We estimate from Fig. 1(a) that $\delta_1 \approx 4$. The real roots of the cubic polynomial in Eq. (9) predict the frequencies of dispersive waves as $\Omega/(2\pi) = 5.1490, 7.2116, -4.1841$ and -5.4178 for $m = 0, 1, -1$, and -2, respectively. These values agree reasonably well with the frequencies of the dispersive waves in Fig. 1(b).

As seen in Fig. 1, the shortest fundamental soliton, created after the fission of a third-order soliton, undergoes a much larger RIFS inside a GRIN fiber compared to a single-mode fiber. The same effect occurs for other values of the soliton-order N. To quantify the magnitude of this enhancement, we plot in Fig. 2, the normalized RIFS, $|\Delta\nu|T_0$, as a function of z/L_D for $N = 2$ and 3 in both types of fibers. The solid dots show the numerical data obtained by isolating the spectrum of the shortest soliton. As seen in Fig. 2, the RIFS is enhanced considerably in the case of a GRIN fiber for both the second- and third-order solitons. The enhancement factor exceeds 2 in both cases even for $C = 0.5$ and is expected to be larger for shorter values of C, as discussed later. This enhancement is a consequence of the spatio-temporal coupling that occurs invariably in the case of GRIN fibers. Periodic spatial contraction of the pulsed Gaussian beam increases the peak power of the soliton in the middle of each self-imaging cycle, thereby enhancing the nonlinear effects in a periodic fashion. Even though the soliton cannot respond to variations occurring at a length scale of 1 mm or less, the effective value of the soliton order increases, resulting in shorter fundamental solitons after

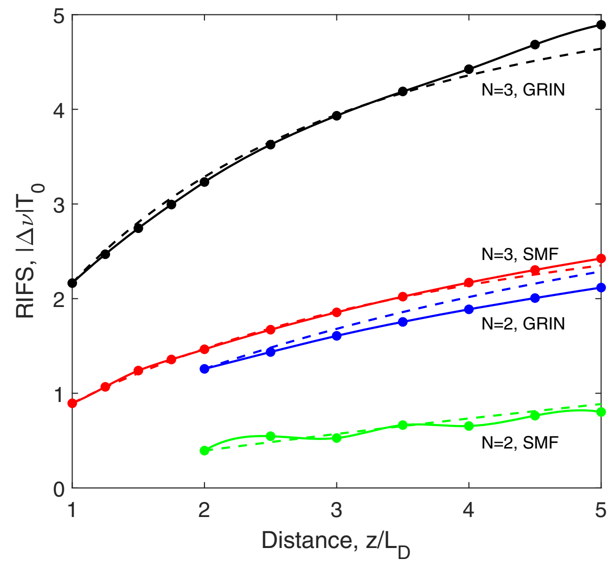

Fig. 2. Magnitude of RIFS plotted over a distance of $5L_D$ for the second- ($N = 2$) and third-order ($N = 3$) input solitons in the cases of GRIN and single-mode fibers (SMF). We used $C = 0.5$ and $q = 100$ for the GRIN fiber. The dashed lines show the predictions of a simple analytic model discussed in the text.

its fission. As the Raman gain is larger for a shorter soliton because of its wider spectrum, the rate of RIFS is also larger for a shorter soliton. This is the reason a larger RIFS occurs in the case of a GRIN fiber for the same input value of N.

An important feature of Fig. 2 is that the RIFS increases with distance sub-linearly for both $N = 2$ and 3, even though a linear dependence is expected from soliton theory based on the assumption that the soliton maintains a constant width [17]. It is easy to deduce that this approximation is not valid when the effects of third-order dispersion are included. As the soliton's spectrum shifts toward the red side, the parameter β_2 begins to change at the center frequency ω_s of the soliton. Using $\beta_2(\omega_s) = \beta_2(\omega_0) + \beta_3(\omega_s - \omega_0)$, we note that the magnitude of $|\beta_2|$ increases for positive values of β_3 used here. From the relation $N^2 = \gamma P_1 T_1^2/|\beta_2|$, with T_1 and P_1 given in Eq. (7) for the shortest soliton created after the fission, it follows that the soliton width T_1 must increase as the RIFS and $|\beta_2|$ increase. Numerical simulations also confirm such an increase.

Although an analytic treatment is not possible, we can estimate the RIFS of the width-varying solitons using the moment method used for perturbed solitons in Ref. [30]. It shows that the RIFS rate $\Delta\nu/dz$ for a soliton of width $T_1(z)$ evolves with distance as

$$\frac{d\Delta\nu}{dz} = \frac{K}{T_1^3}, \tag{10}$$

where K is a constant. We estimate K from the numerical simulations at a distance z_f chosen to be after the fission has occurred and where $T_1(z_f)$ can be estimated from Eq. (7). Since we do not know the exact dependence of T_1 on z, to the first-order in the Taylor expansion, we take it to be linear and use

$$T_1(z) = T_1(z_f)[1 + s(z - z_f)], \tag{11}$$

where the slope s is estimated from the numerical data. Integrating Eq. (10) using $T_1(z)$ from Eq. (11), we obtain

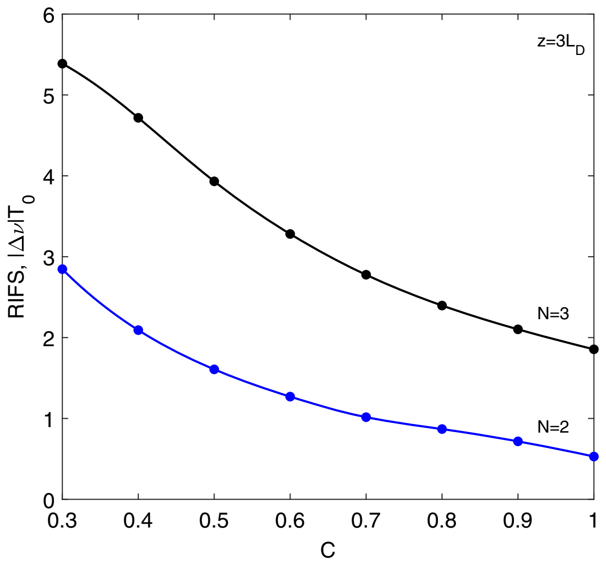

Fig. 3. Magnitude of RIFS plotted as a function of C for a fixed fiber length of $3L_D$ for the second- ($N = 2$) and third-order ($N = 3$) solitons propagating inside a GRIN fiber. The dashed lines show the results obtained for single-mode fibers under identical conditions.

the z dependence of the RIFS. The results are shown in Fig. 2 with the dashed lines, solid lines showing the numerical results. As can be seen, our rough estimate agrees with the simulation results reasonably well.

The results shown in Fig. 2 are for a specific GRIN fiber for which $q = 100$ and $C = 0.5$. We briefly discuss how the RIFS enhancement is affected when these parameters are varied. It is easy to deduce that the results do not depend on the precise value of q as long as the self-imaging period of the GRIN fiber is much shorter than the dispersion length, resulting in $q > 10$. This is not the case for the C parameter. In fact, we expect the RIFS to depend considerably on this parameter because the Gaussian beam is compressed more and more during each self-imaging period as C becomes smaller. The results shown in Fig. 3 confirm this expectation. As seen there, the RIFS increases rapidly as C decreases and is always larger for a GRIN fiber compared to its value at $C = 1$ for which the beam width does not oscillate.

In conclusion, we have investigated how the intrapulse Raman scattering and third-order dispersion affect the propagation of optical pulses inside GRIN fibers by solving an effective NLS equation that includes the spatial self-imaging effects through a periodically varying effective mode area. Numerical simulations are used to show that the RIFS of the shortest fundamental soliton created after the fission process is enhanced considerably inside GRIN fibers compared to single-mode fibers for the same value of the input soliton order N. We also discuss how a larger beam-width reduction during each self-imaging cycle leads to a larger RIFS.

Funding. National Science Foundation (NSF) (ECCS-1505636).

REFERENCES

1. D. J. Richardson, J. M. Fini, and L. E. Nelson, Nat. Photonics **7**, 354 (2013).
2. F. Poletti and P. Horak, J. Opt. Soc. Am. B **25**, 1645 (2008).
3. A. Mafi, J. Lightwave Technol. **30**, 2803 (2012).
4. Z. Liu, L. G. Wright, D. N. Christodoulides, and F. W. Wise, Opt. Lett. **41**, 3675 (2016).
5. K. Krupa, A. Tonello, B. M. Shalaby, M. Fabert, A. Barthelemy, G. Millot, S. Wabnitz, and V. Couderc, Nat. Photonics **11**, 237 (2017).
6. S. Longhi, Opt. Lett. **28**, 2363 (2003).
7. K. Krupa, A. Tonello, A. Barthelemy, V. Couderc, B. M. Shalaby, A. Bendahmane, G. Millot, and S. Wabnitz, Phys. Rev. Lett. **116**, 183901 (2016).
8. W. H. Renninger and F. W. Wise, Nat. Commun. **4**, 1719 (2013).
9. S.-S. Yu, C.-H. Chien, Y. Lai, and J. Wang, Opt. Commun. **119**, 167 (1995).
10. S. Raghavan and G. P. Agrawal, Opt. Commun. **180**, 377 (2000).
11. A. S. Ahsan and G. P. Agrawal, Opt. Lett. **43**, 3345 (2018).
12. L. G. Wright, D. N. Christodoulides, and F. W. Wise, Nat. Photonics **9**, 306 (2015).
13. K. Krupa, C. Louot, V. Couderc, M. Fabert, R. Guenard, B. M. Shalaby, A. Tonello, D. Pagnoux, P. Leproux, A. Bendahmane, R. Dupiol, G. Millot, and S. Wabnitz, Opt. Lett. **41**, 5785 (2016).
14. G. Lopez-Galmiche, Z. Sanjabi Eznaveh, M. A. Eftekhar, J. Antonio Lopez, L. G. Wright, F. Wise, D. Christodoulides, and R. Amezcua Correa, Opt. Lett. **41**, 2553 (2016).
15. M. A. Eftekhar, L. G. Wright, M. S. Mills, M. Kolesik, R. Amezcua Correa, F. W. Wise, and D. N. Christodoulides, Opt. Express **25**, 9078 (2017).
16. G. P. Agrawal, *Nonlinear Fiber Optics*, 5th ed. (Academic, 2013).
17. J. P. Gordon, Opt. Lett. **11**, 662 (1986).
18. J. H. Lee, J. van Howe, C. Xu, and X. Liu, IEEE J. Sel. Top. Quantum Electron. **14**, 713 (2008).
19. Y. Tang, L. G. Wright, K. Charan, T. Wang, C. Xu, and F. W. Wise, Optica **3**, 948 (2016).
20. B. Li, M. Wang, K. Charan, M.-J. Li, and C. Xu, Opt. Express **26**, 19637 (2018).
21. M. Conforti, C. M. Arabi, A. Mussot, and A. Kudlinski, Opt. Lett. **42**, 4004 (2017).
22. K. J. Blow and D. Wood, IEEE J. Quantum Electron. **25**, 2665 (1989).
23. J. Hult, J. Lightwave Technol. **25**, 3770 (2007).
24. L. G. Wright, W. H. Renninger, D. N. Christodoulides, and F. W. Wise, Opt. Express **23**, 3492 (2015).
25. Z. Zhu, L. G. Wright, D. N. Christodoulides, and F. W. Wise, Opt. Lett. **41**, 4819 (2016).
26. M. Conforti, S. Trillo, A. Mussot, and A. Kudlinski, Sci. Rep. **5**, 9433 (2015).
27. M. Conforti, S. Trillo, A. Kudlinski, and A. Mussot, IEEE Photon. Technol. Lett. **28**, 740 (2016).
28. L. G. Wright, S. Wabnitz, D. N. Christodoulides, and F. W. Wise, Phys. Rev. Lett. **115**, 223902 (2015).
29. M. Conforti and S. Trillo, Opt. Lett. **38**, 3815 (2013).
30. J. Santhanam and G. P. Agrawal, Opt. Commun. **222**, 413 (2003).